Optical Spectra of Protected Diamine 10-Bond-Bridged Intervalence Radical Cations Related to N , N , N ‘ N ‘-Tetraalkylbenzidine

ARTICLE *in* THE JOURNAL OF ORGANIC CHEMISTRY · JUNE 2006

Impact Factor: 4.72 · DOI: 10.1021/jo060466l · Source: PubMed

5 AUTHORS, INCLUDING:

Stephen F Nelsen
University of Wisconsin–Madison
118 PUBLICATIONS **2,249** CITATIONS
SEE PROFILE

Jeffrey I Zink
University of California, Los Angeles
470 PUBLICATIONS **22,181** CITATIONS
SEE PROFILE

JOC*Article*

Optical Spectra of Protected Diamine 10-Bond-Bridged Intervalence Radical Cations Related to *N,N,N′N′*-Tetraalkylbenzidine

Stephen F. Nelsen,*,† Yun Luo,† Michael N. Weaver,† Jenny V. Lockard,‡ and Jeffrey I. Zink‡

Department of Chemistry, University of Wisconsin, 1101 University Avenue, Madison, Wisconsin 53706-1396, and the Department of Chemistry and Biochemistry, University of California, Los Angeles, California 90095

nelsen@chem.wisc.edu; zink@chem.ucla.edu

Received March 3, 2006

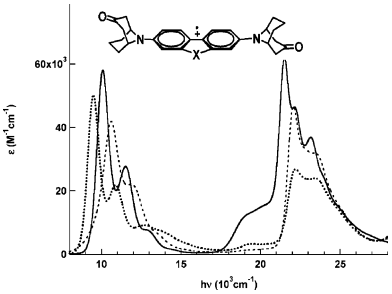

The optical absorption spectra of the delocalized intervalence radical cations of seven o,o′-linked benzidine derivatives that have the nitrogens protected as 9-(9-aza-bicyclo[3.3.1]nonan-3-one) derivatives are discussed and compared with that of the *p*-phenylene radical cation. The linking units are CH_2, CH_2CH_2, NMe, S, SO_2, and C═O, and we also studied H,H (the unlinked benzidine). The lowest-energy absorption band is assigned as the transition from the antibonding combination of symmetrical N and aromatic orbitals to the antibonding combination of the antisymmetric N and aromatic orbitals using TD-DFT calculations, and a good correlation between the observed transition energies and those calculated using the simple Koopmans theorem-based "neutral in-cation geometry" calculations on the UB3LYP/6-31G* structures is found. The use of the two-state model that equates the electronic interaction through the bridge between the amino groups with half of the lowest transition energy is seriously incorrect for these and other delocalized intervalence compounds. The problem of extracting the electronic interactions that actually are involved from calculated transition energies is discussed.

Introduction

We recently discussed the optical absorption, emission, and resonance Raman spectra of the five-bond-bridged protected tetraalkyl-*p*-phenylenediamine radical cation derivative **1,4-PH**$^+$.[1] It is a delocalized (Robin−Day[2] Class III) symmetrical

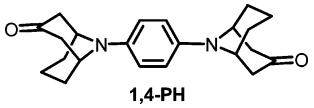

1,4-PH

intervalence compound. Symmetrical intervalence compounds have two identical charge-bearing units (**M**, in this case, the 9-(9-azabicyclo[3.3.1]nonan-3-one) group) symmetrically attached to a bridge (**B**, in this case, the *p*-phenylene aromatic group, **PH**) and are at an oxidation level for which the charges on **M** might be different. **1,4-PH**$^+$ has delocalized charge and might be abbreviated $^{1/2+}$**M-B-M**$^{1/2+}$, although some of the charge is delocalized onto the C_6H_4 bridge. We analyzed the electronic interaction between the amino groups of **1,4-PH**$^+$ using the usual Marcus−Hush two-state model,[3,4] which we believe Creutz first explicitly noted requires that the off-diagonal coupling term V (which is also often called H_{ab}) is one-half of

† University of Wisconsin.
‡ University of California, Los Angeles.

(1) Bailey, S. E.; Zink, J. I.; Nelsen, S. F. *J. Am. Chem. Soc.* **2003**, *125*, 5939−5947.
(2) Robin, M. B.; Day, P. *Adv. Inorg. Chem. Radiochem.* **1967**, *10*, 247−422.
(3) (a) Marcus, R. A. *J. Chem. Phys.* **1956**, *24*, 966−978. (b) Marcus, R. A.; Sutin, N. *Biochim. Biophys. Acta* **1985**, *811*, 265−322.

10.1021/jo060466l CCC: $33.50
Published on Web 05/02/2006

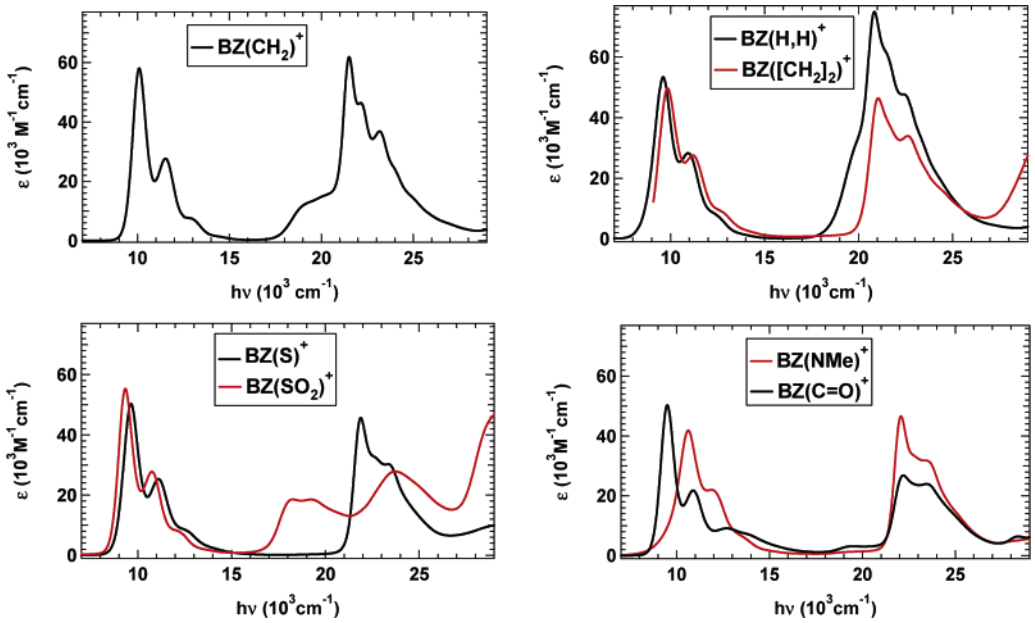

FIGURE 1. Optical spectra of seven protected aromatic diamine radical cations in acetonitrile, at room temperature.

the intervalence band transition energy for a delocalized case.[5] Because **1,4-PH**$^+$ shows vibrational fine structure and the band maximum corresponds to the 0,0 band, we thought that *V* could be determined especially accurately for it and related compounds and have discussed both observed and calculated structural and solvent effects on *V* using it and related compounds.[6,7] This two-state model interpretation is routinely used in calculations of *V*, often with reference to pioneering papers by Larsson.[8] This work demonstrates why the two-state model, which as shown by three recent reviews is still being used for delocalized intervalence compounds,[9] is inadequate for consideration of the optical spectra of these and other delocalized intervalence compounds.

The optical spectra of seven protected diaminoaromatic radical cations that have nine-bond bridges between the amino groups are studied in this work. They are mostly linked between the o,o′ positions of a benzidine framework, and for convenience, we will designate them by the linking unit, that is, **BZ(X)** in the structure below, **X = H,H** for the parent benzidine

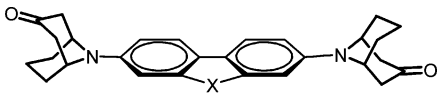

BZ(X)

compound, and **X = [CH$_2$]$_2$** for its diaminodihydrophenanthrene-bridged analogue. Like **1,4-PH**$^+$, **BZ(X)**$^+$ are delocalized

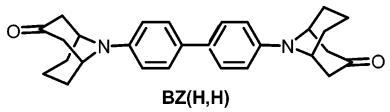

BZ(H,H)

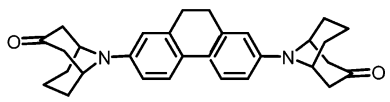

BZ([CH$_2$]$_2$)

intervalence compounds, and we discuss here the origin of the low-energy absorption bands in these systems. **BZ(H,H)** and **BZ([CH$_2$]$_2$)** are the only compounds studied that can twist significantly at the central bond,[10] as the five-membered rings of the **X = CH$_2$**, **CO**, **NMe**, **S**, and **SO$_2$**-linked compounds prevent this twisting.

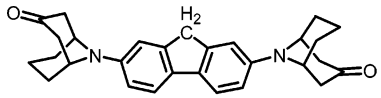

BZ(CH$_2$)

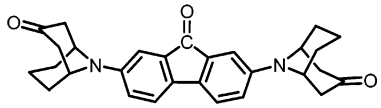

BZ(CO)

Results

The absorption spectra (room temperature, acetonitrile) of the seven **BZ(X)**$^+$ compounds are displayed in pairs in Figure 1. Despite the different π systems involved in some cases, all of these **BZ(X)**$^+$ compounds show first bands near 10 000 cm^{-1} (we will refer to their band maximum as E_{a1}) as well as a second band (maximum E_{a2}) showing at least some vibrational fine structure that comes in the 21 000−22 000 cm^{-1} range (except for the SO_2 bridged compound, which shows a second band near 18 000 cm^{-1}). There are also smaller bands for most

(4) (a) Hush, N. S. *Trans. Faraday Soc.* **1961**, *57*, 557−580. (b) Hush, N. S. *Prog. Inorg. Chem.* **1967**, *8*, 391−444. (c) Hush, N. S. *Coord. Chem. Rev.* **1985**, *64*, 135−57.

(5) Creutz, C. *Prog. Inorg. Chem.* **1983**, *30*, 1−73.

(6) Nelsen, S. F.; Tran, H. Q. *J. Am. Chem. Soc.* **1998**, *120*, 298−304.

(7) Nelsen, S. F.; Tran, H. Q. *J. Phys. Chem. A* **1999**, *103*, 8139−8144.

(8) (a) Broo, A.; Larsson, S. *Chem. Phys.* **1990**, *148*, 103−115. (b) Braga, M.; Broo, A.; Larsson, S. *Chem. Phys.* **1991**, *156*, 1−9.

(9) (a) Brunschwig, B. S.; Creutz, C.; Sutin, N. *Chem. Soc. Rev.* **2002**, *31*, 168−184. (b) Demadis, K. D.; Hartshorn, C. M.; Meyer, T. J. *Chem. Rev.* **2001**, *101*, 2655−2685. (c) Nelsen, S. F. *Chem.−Eur. J.* **2000**, *6*, 581−588.

(10) The calculated twist at the central bond of **BZ(H,H)** is 16.1° (using UB3LYP/6-31G* calculations; 12.3° by AM1), and that of **BZ([CH$_2$]$_2$)** is 18.5° (using UB3LYP/6-31G*; 14.5° by AM1).

TABLE 1. Absorption Maxima (cm^{-1}) for $BZ(X)^+$ in CH_3CN at Room Temperature

compound	E_{a1} obsd	E_{a2} obsd
BZ(SO$_2$)$^+$	9340	18240
BZ(CO)$^+$	9490	22200
BZ(S)$^+$	9640	21800
BZ(CH$_2$)$^+$	10100	21500
BZ(NMe)$^+$	10630	22080
BZ([CH$_2$]$_2$)$^+$	9840	21050
BZ(H,H)$^+$	9600	20850

compounds near the low-energy edge of the second major band. The band maxima for the first and second absorption bands are summarized in Table 1.

Discussion

1. TD-DFT Calculations. Previous work[6] showed that the N-methylated systems have first band maxima that are only slightly higher than those for the bicyclononanone-protected systems, by 54 cm^{-1} for **TMPD**$^+$ and by 17 cm^{-1} for **TMB**$^+$ (compared to the result reported in Table 1 for **BZ(H,H)**$^+$). We

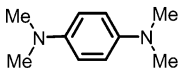

TMPD

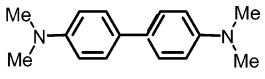

TMB [MBZ(H,H)]

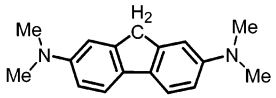

MBZ(CH$_2$)

report results here for hybrid density functional theory calculations (UB3LYP, called DFT for brevity), carried out using the 6-31G* basis set for dimethylamino-substituted compounds (abbreviated **MBZ(X)**) as well as for the 9-azabicyclo[3.3.1]-nonyl **BZ** compounds that have the carbonyl group replaced by CH_2 (abbreviated **3BZ(X)**). The nature of the low-energy transitions for two of the specific compounds considered here has been considered using time-dependent density functional theory calculations (TD-DFT)[11] as summarized in Table 2 (corresponding data for **MBZ(CH$_2$)**$^+$ appear in Supporting Information). In other work, **TMPD**$^+$ was calculated with both 6-31G* and 6-31+G* basis sets (results not shown here), and the changes were found to be small compared to errors in the calculations; therefore, the DFT calculations for the larger benzidine compounds were only carried out using the 6-31G* basis set.

The energy levels and orbital drawings for **MBZ(CH$_2$)**$^+$ are shown in Figure 2. There are no two-electron "filled orbitals" for open-shell systems. The doubly occupied orbitals that are used in a restricted open-shell Hartree−Fock (ROHF) treatment are actually split into α and β spin sets by the unpaired electron. The sizes of the splittings vary considerably from orbital to orbital. The transition energies are very far from the energy differences that are calculated between the orbitals to which they are assigned both because occupation of an orbital has a large effect on its energy and because of the configuration of the interaction; many optical transitions do not correspond to simple promotions of one electron to an unfilled orbital, but to combinations of such processes. However, the TD-DFT calculations get the lower-energy transitions here as involving predominantly simple promotions from filled β to the β lowest-unoccupied (lumo) level (68β for **BZ(CH$_2$)**$^+$) or, using the language of ROHF calculations, from filled orbitals to the somo. Such transitions are between the Koopmans (also called *G*(round) and *A*-type) configurations;[12] we will follow Bally in calling such transitions Hoijtink type *A* transitions.[13]

2. Koopmans-Based Calculations. We also calculated the type *A* transition energies using the far less computationally expensive neutral in-cation geometry (NCG) method[14] and included them at the right side of Table 2. NCG calculations involve performing a single SCF at the geometry of the radical cation using a zero charge, so the system is closed shell and does have two-electron orbitals. This makes both orbitals involved in these transitions have two electrons. When an optical absorption in a radical cation is caused by simple excitation of an electron from a doubly filled orbital to the somo, the orbital separation in an NCG calculation is an excellent approximation to the ROHF transition energy. We showed previously that the calculated energies for the first transition obtained by the NCG method using simple AM1 calculations give rather good correlations with experimental data for diamino-substituted aromatic symmetrical intervalence radical cations, although the calculated values were high, by 2650 cm^{-1} for **TMPD**$^+$, by 3700 cm^{-1} for **1,4-PH**$^+$, and by 800 cm^{-1} for **TMB**$^+$.[6] Not surprisingly, the DFT NCG calculations give answers closer to experiment than the AM1 values, and we will only use DFT numbers here.

In type *B* transitions (also called non-Koopmans, NK, by Bally),[12] an electron is promoted from the somo to a virtual orbital using an ROHF basis or from the α homo to an α unoccupied MO of an open-shell DFT calculation. Although type *A* transitions are usually the lowest in energy for radical cations, a type *B* transition is calculated to be responsible for the second large band in the optical spectra observed for the compounds studied here and to be the fifth highest transition for **MBZ(CH$_2$)**$^+$, so one needs to calculate type *B* as well as type *A* transitions to understand radical ion optical spectra. We recently suggested using a simple Koopmans-based calculation for type *B* transitions. For a radical anion, the somo and lumo orbitals are at the same occupancy (both empty) for the "neutral in-anion geometry" (NAG) calculation.[15] For radical cations, this situation corresponds to "dication in-cation geometry" (DCG). Results of DCG calculations for the first type *B* transition are also included in Table 2. It is very important to have the electron correlation that is present in (U)B3LYP calculations; NCG/DCG calculated transition energies using HF/6-31G* either at HF/6-31G* or UB3LYP/6-31G* geometries are considerably different and appear to be of little use when compared with experimental transition energies. It should be noted that the calculated intensities for both TD-DFT and Koopmans-based calculations only refer to the ground-state

(11) (a) Burke, K.; Gross, E. K. U. In *Density Functionals: Theory and Applications*; Joubert, D., Ed.; Springer: Berlin, 1998; pp 116−146. (b) Casida, M. E.; Jamorski, C.; Casida, K. C.; Salhub, D. R. *J. Chem. Phys.* **1998**, *108*, 4439. (c) Stratmann, R. E.; Scuseria, G. E.; Frisch, M. J. *J. Chem. Phys. Chem.* **1998**, *109*, 8218−8224.

(12) Bally, T. In *Radical Ionic Systems*; Lund, A., Shiotani, M., Eds.; Kluwer: Dortrecht, 1991; pp 3−54.

(13) (a) Hoijtink, G. J.; Weijland, W. P. *Recl. Trav. Chim.* **1957**. *76*, 836−838. (b) Buschow, K. J. J.; Dieleman, J.; Hoijtink, G. J. *Mol. Phys.* **1963−1964**, *7*, 1−9.

(14) Nelsen, S. F.; Blackstock, S. C.; Yumibe, N. P.; Frigo, T. B.; Carpenter, J. E.; Weinhold, F. *J. Am. Chem. Soc.* **1985**, *107*, 143−149.

(15) Nelsen, S. F.; Konradsson, A. E.; Telo, J. P. *J. Am. Chem. Soc.* **2005**, *127*, 920−925.

TABLE 2. TD-DFT B3LYP Calculations[a] of the Five Lowest-Energy Transitions for 3BZ(CH$_2$)$^+$, Compared with Koopmans-Based NCG/DCG Results

	TD-DFT			Koopmans-based	
transition	$h\nu$ (cm^{-1})[a]	f[b]	assignment	$h\nu$ (cm^{-1})[a]	f[b]
1	11880	0.51	(81%) 111β→112β A_1 (11%) 112α→113α B_1	10600 A_1	.3012
2	19490	0.0003	(100%) 110β→112β A_2	18870 A_2	.0012
3	21050	0.0040	(87%) 112α→113α A_3 (13%) 108β→109β A_4	20310 A_3	.0004
4	23590	0.00	(79%) 108β→112β A_4 (11%) 109β→112β A_3 (7%) 111α→113α C	24199 A_4	.0059
5	26060	0.84	(81%) 112α→113α B_1 plus 7 other minor ones	24780 B_1 31700 A_5	.2773 .0096

[a] Calculated with a 6-31G* basis set. [b] Oscillator strength.

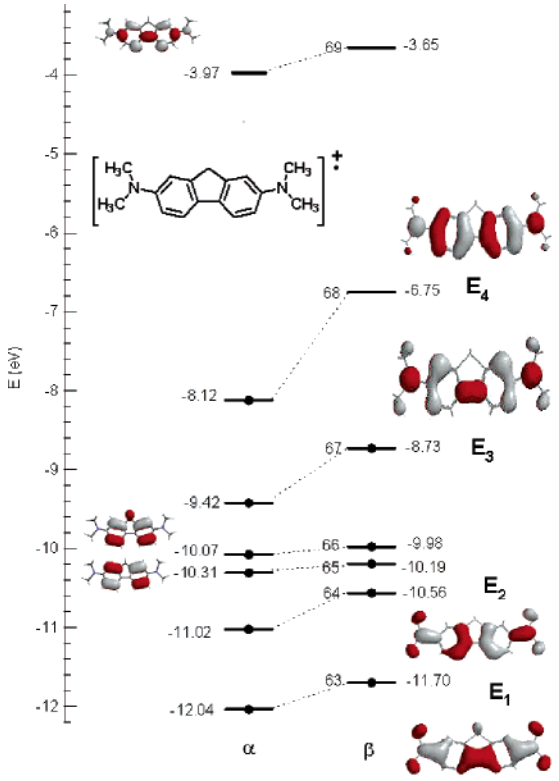

FIGURE 2. Pictorial representation of the upper orbitals for **MBZ(CH$_2$)$^+$** from a UB3LYP/6-31G* calculation.

geometry, whereas real molecules sample a much larger portion of their excited state surface in vertical transitions, causing strongly forbidden absorptions to be often calculated with intensities that are significantly too low. The calculated transition energies are for the gas phase, which will tend to make them too high. Type *C* transitions that correspond to filled orbital to virtual ones also appear in optical spectra of radical ions,[12] but their energies cannot be predicted using the Koopmans-based method.

The TD-DFT and Koopmans-based calculated spectra of **MBZ(CH$_2$)$^+$** and **3BZ(CH$_2$)$^+$** are compared with the observed spectra of **BZ(CH$_2$)$^+$** in Figure 3. Although they are quite similar, calculations using the larger alkyl groups that are closer to the ones used for the experiment do give results that are closer to the experimental values. We note that TD-DFT shows significant amounts of configuration interaction as being present. Even for the lowest-energy transition, it obtains about an 11% admixture of B_1 with the predominant A_1 character; both the orbitals involved have the same b_1 symmetry for the C_{2v} **MBZ(CH$_2$)$^+$** calculation. The predominately B_1 transition that is principally responsible for the second absorption band is calculated by TD-DFT to be even more seriously mixed, with seven or eight type *C* transitions contributing. Mixing with higher-energy transitions should lower the energy, and perhaps the reason that the Koopmans-based calculation is too high for the higher-energy transition is this mixing, which is completely ignored in the Koopmans-based calculations. The calculated $h\nu$ values are about 500 and 3300 cm^{-1} higher than the 0,0 band maxima observed for the first and second absorption bands using Koopmans-based calculations. The second band is further off, possibly because it really does have more extensive configuration interaction. The TD-DFT calculations are further from experiment, 1000 and 4400 cm^{-1} higher. It should be noted that, despite the fact that TD-DFT uses complex algorithms that employ open-shell calculations and configuration interaction, the Koopmans-based calculations that ignore configuration interaction produce transition energy values that are closer to the experimental ones than are TD-DFT calculations and give rather similar predicted intensities. Slightly better Koopmans-based than TD-DFT transition energies have been obtained for the great majority of the radical ions that we have investigated thus far.

The effect of changing the nature of the linking ring is calculated rather well, as shown in Figure 4, where calculations on the **3BZ(X)$^+$** compounds are compared with experimental data for their 3-keto analogues, **BZ(X)$^+$**. The root-mean-square deviation from the observed values is 490 cm^{-1}, which is smaller than the 900 cm^{-1} value obtained for calculations on the **Me$_2$N** derivatives (see the Supporting Information for these data). The compounds that twist about the central bond, **MBZ(H,H)$^+$** and **MBZ([CH$_2$]$_2$)$^+$**, are not really calculated consistently with the other compounds because of the very soft twist about the central C−C bond.[10] Changing the twist of **MBZ(H,H)** from 16.1° to 0° increases the energy by less than *kT*, 0.15 kcal/mol. The calculated transition energy would have to be Boltzmann-weighted and averaged over the energy surface for twisting to produce a more significant calculated number,[16] a procedure that would be costly and is rather clearly not justified for these data. The NCG calculations are quite successful at estimating the effect on the band position of changing the linking substituents of the bridge to be electron releasing and are somewhat less successful but still rather good for the electron-

(16) Nelsen, S. F.; Frigo, T. B.; Kim, Y. *J. Am. Chem. Soc.* **1989**, *111*, 5387−5397.

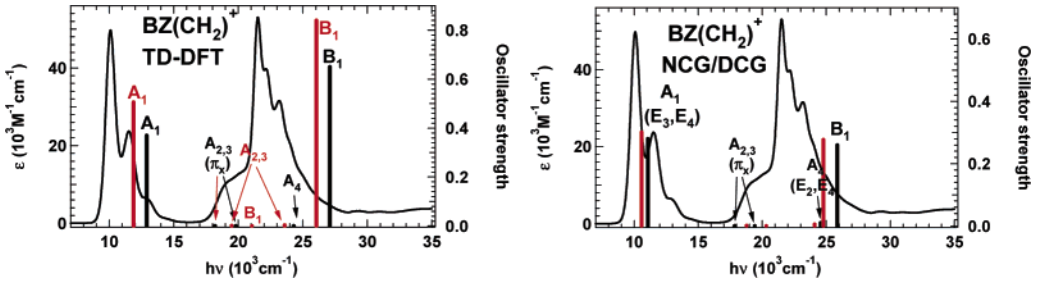

FIGURE 3. Calculated transitions for **MBZ(CH$_2$)**$^+$ (black sticks) and **3BZ(CH$_2$)**$^+$ (red sticks) superimposed on the observed spectra of **BZ-(CH$_2$)**$^+$. Left panel: TD-DFT calculations. Right panel: Koopmans-based NCG/DCG calculations.

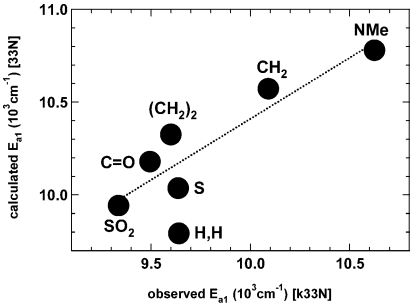

FIGURE 4. Plots of the calculated A_1 transition for **3BZ(X)**$^+$ vs observed E_{a1} for **BZ(X)**$^+$. The line shown is a regression line through the planar π systems.

withdrawing CO and SO_2. We therefore feel justified in using these calculations to consider how changing the linking unit **X** affects electronic coupling in these compounds, which is considered in the next section.

3. Neighboring Orbital Model. To relate the observed optical spectrum to electronic couplings involving the **M** groups and the aromatic bridge orbitals, it is necessary to convert adiabatic state energy differences, which have the electronic interaction intact, back to the hypothetical diabatic energy levels of the **M** groups and bridge orbitals, in the absence of any electronic interaction between them. To do this, we consider the assignment of the transitions involving nitrogen lone pairs, an aryl π system interaction for these compounds using a simple Hoffmann-type analysis,[17] in which only orbitals of proper symmetry that are closest in energy are considered to mix significantly. The molecular orbitals involved in these transitions may be constructed by mixing diabatic **M** combination orbitals that are dominated by symmetric and antisymmetric combinations of the nitrogen p lone pairs (**N**) with the aryl ring π orbitals, shown in Figure 5 for D_{2h} (planar) biphenyl for simplicity.

The aryl diabatic orbitals with a_u and b_{1g} symmetry, shown as the pair in the center of the diagram, cannot mix significantly with the **N** orbitals because they are antisymmetric with respect to the *xy* plane, which places a node through the CN bonds. These two biphenyl orbitals are similar in energy because they differ only by a nonbonded C_2,C_2', C_6,C_6' overlap. The symmetric combination of **N** orbitals can only mix with the filled bridge orbital that is symmetric with respect to the *yz* mirror plane (the b_{3u} orbital in Figure 2). The antisymmetric combination of **N** orbitals can only mix with the filled bridge orbital that is antisymmetric with respect to the *yz* mirror plane (the b_{2g} orbital in Figure 2). This leads to four adiabatic combination orbitals that are either bonding or antibonding at the **M**−**B** bonds, as indicated in cartoon form in Figure 6 for the case of the **BZ(X)** radical cations studied here, where both the upper and lower aryl orbitals are filled and the upper orbital is antisymmetric. In this paper, we assume that the local symmetry for all of the benzidine molecules contains the *yz* mirror plane. The symmetric and asymmetric diabatic nitrogen lone pair combinations are the same energy, H_{bb}, because the **N** p lone pair orbitals have negligible direct overlap and by symmetry will only mix with aryl orbitals of appropriate symmetry. Mixing is assumed to be proportional to $1/\Delta E$, so V^U will be larger than V^L for the case shown, where ΔE^U is smaller than ΔE^L. The energy order will reliably be that shown. The cartoon is drawn using an ROHF basis, with two-electron filled orbitals. The case shown has both aryl orbitals occupied, as occurs for the benzidine derivatives, so these compounds have seven-electron neighboring orbital systems, as indicated. The ground-state configuration is $(E_1)^2(E_2)^2(E_3)^2(E_4)^1$, the first neighboring orbital excited state is $(E_1)^2(E_2)^2(E_3)^1(E_4)^2$, and so on. The state energies lie in the order opposite to that of the orbital energies, and we will discuss them in terms of the orbitals from which electrons are excited to the E_4 somo. The mathematics for obtaining the adiabatic orbitals in terms of the diabatic orbitals appear elsewhere.[18] We designate the diabatic energies as H and the electronic couplings as V and use superscripts U (upper) and L (lower) to distinguish the neighboring bridge orbitals (because symmetry designations are inconvenient because they switch depending upon the bridge size). The result is simply that, for two two-state models[3] which are related by having the same H_{bb} energy (eqs 1−4), where $\Delta E^U = H^U - H_{bb}$ and $\Delta E^L = H_{bb} - H^L$.

$$E_1 = \frac{1}{2}(H^L + H_{bb} - [(\Delta E^L)^2 + 4(V^L)^2]^{1/2}) \quad (1)$$

$$E_3 = \frac{1}{2}(H^L + H_{bb} + [(\Delta E^L)^2 + 4(V^L)^2]^{1/2}) \quad (2)$$

$$E_2 = \frac{1}{2}(H_{bb} + H^U - [(\Delta E^U)^2 + 4(V^U)^2]^{1/2}) \quad (3)$$

$$E_4 = \frac{1}{2}(H_{bb} + H^U + [(\Delta E^U)^2 + 4(V^U)^2]^{1/2}) \quad (4)$$

These equations may be solved if the relationship between V^L and V^U is known. The proper evaluation of the proportionality constant between V values and energy differences ΔE is basically an unsolved problem.[19] The approximation made for this work is that the coupling is inversely proportional to the

(17) Hoffmann, R. *Acc. Chem. Res.* **1971**, *4*, 1−9.

(18) Nelsen, S. F.; Weaver, M. N.; Luo, Y.; Lockard, J. V.; Zink, J. I. *Chem. Phys.*, in press.

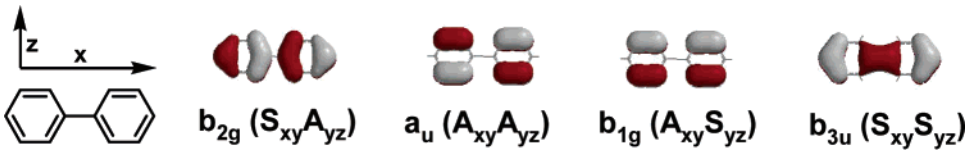

FIGURE 5. π orbital electron density diagrams for the upper filled π orbitals of planar biphenyl.

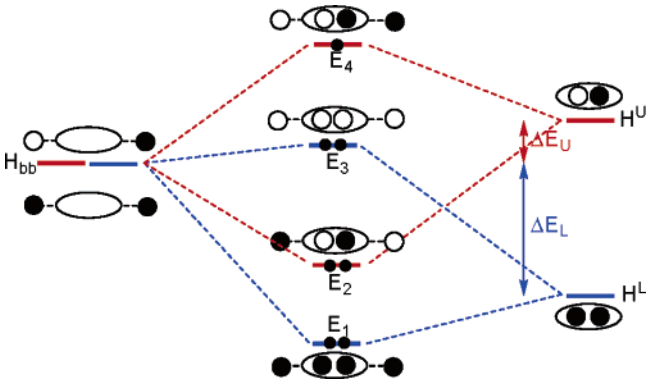

FIGURE 6. Diagrammatic representation of diabatic nitrogen and aromatic combination orbitals for **BZ(X)** derivatives.

difference in energy between the two diabatic orbitals that are mixing, i.e., eq 5.

$$\frac{V^{\mathrm{L}}}{V^{\mathrm{U}}} = \frac{\Delta E^{\mathrm{U}}}{\Delta E^{\mathrm{L}}} \tag{5}$$

It is convenient to consider the inverse proportionality relationship between V and ΔE that is shown in eq 5 as the diabatic energy difference/electronic coupling product ratio R of eq 6, because R should be near 1 for acceptable solutions to the neighboring orbital problem.

$$R = \frac{(H_{\mathrm{bb}} - H^{\mathrm{U}})V^{\mathrm{U}}}{(H^{\mathrm{L}} - H_{\mathrm{bb}})V^{\mathrm{L}}} \tag{6}$$

Although $R \sim 1$ is only an approximation because of differential overlap effects, mathematically acceptable solutions to eqs 1−5 for large portions of the parameter range that produces real solutions have R values that lie far from 1, so they may be excluded easily.

To evaluate the electronic couplings of neighboring orbital systems, it is necessary to obtain the adiabatic orbital energies, E_1−E_4, of Figure 6. The only neighboring orbital transition that can be clearly located in the optical spectra is E_{a1}, corresponding to $E_4 - E_3$ (which is the A_1 transition for these compounds). It may be noted in Table 2 that although the $E_2 \rightarrow E_4$ transition for **MBZ(CH$_2$)**$^+$ is not completely forbidden because the transition dipoles are not exactly at 180° it is still calculated to be far smaller than the allowed A_1 transition and only slightly more intense than larger forbidden π_x transitions. It certainly cannot be located in the experimental spectrum because of other transitions in this region, although it probably contributes to the bump before the intense B_1 transition of **BZ(CH$_2$)**$^+$. The E_1,E_4 energy separation (calculated as the A_5 transition) was also predicted to be too weak to observe. We therefore turn to Koopmans-based NCG calculations to consider the neighboring orbital transitions of the **BZ(X)** radical cations, shown in Table 3 for the UB3LYP/6-31G* geometries. An advantage of Koopmans-based calculations is that all of the type *A* and *B* transitions are produced about an order of magnitude more rapidly than a five-state TD-DFT calculation for these molecules. This is important for considering a neighboring orbital analysis because rather high-energy transitions are involved for $E_1 \rightarrow E_4$ and many more than five transitions would have to be calculated to use TD-DFT to estimate the transition energies. Furthermore, the Koopmans-based model is much simpler and is appropriate for implementing our simple neighboring orbital model. For the purpose of estimating the size of electronic couplings, it is not the complex configuration interaction that leads to the observed transition energies that is important but how to simplify the complex output of electronic structure calculations to extract such couplings.

TABLE 3. DFT-NCG Orbital Energies for 33N-Substituted Compounds 3BZ(X) (cm^{-1}) Compared to the Observed First Band Maximum for the k33N-Substituted Compounds (E_{a1}(BZ**$^+$))**

X of **3BZ(X)**$^+$	E_4	E_3	E_2	E_1	E_{a1}(**BZ**$^+$)	ΔE^a
NMe	≡0	−10780	−24062	−30110	10630	150
CH$_2$[b]	≡0	−10573	−23865	−31699	10100	473
[CH$_2$]$_2$	≡0	−10326	−23507	−31437	9600	726
H,H	≡0	−9793	−23724	−31134	9640	153
S	≡0	−10037	−24090	−29357	9840	197
CO	≡0	−10180	−24003	−31624	9490	690
SO$_2$	≡0	−9943	−23594	−27267	9340	603

[a] Difference between E_{a1}(**BZ**$^+$) and the calculated transition energy, $E_4 - E_3$. [b] The geometry was reoptimized for the DIMO calculation of Table 2, leading to changes in the neighboring orbital transition energies of ≤240 cm^{-1}.

4. Estimation of Electronic Couplings. The lowest-energy electronic transition for these compounds (E_{a1}) is twice the electronic coupling, $2H_{ab}$, for this Class III system according to the widely used two-state model. The logarithm of lowest transition energy does drop approximately linearly with increasing number of bonds in the bridge in many cases. This is the expected behavior for H_{ab}, encouraging the assumption that the transition energy should be equated with $2H_{ab}$. We recently pointed out that the linearity with the number of connecting bonds breaks down for certain Class III dinitroaromatic radical anions, most clearly the 1,5-dinitronaphthalene derivative.[20] Because the intervalence transition for **BZ(X)**$^+$ is the A_1 transition, which is between orbitals of different symmetries, it obviously cannot correspond to the $2H_{ab}$ separation between the energy levels of a single two-state model, to which it is attributed if the two-state model is applied to a Class III intervalence compound. In this section, we discuss whether considering the intervalence transition energy to be directly proportional to the electronic coupling is useful for **BZ(X)**$^+$.

(19) For a discussion in the context of the ethane rotational barrier problem, see: Weinhold, F. *Angew. Chem. Int. Ed.* **2003**, *42*, 4188−4194.

(20) Nelsen, S. F.; Weaver, M. N.; Zink, J. I.; Telo, J. P. *J. Am. Chem. Soc.* **2005**, *127*, 10611−10622.

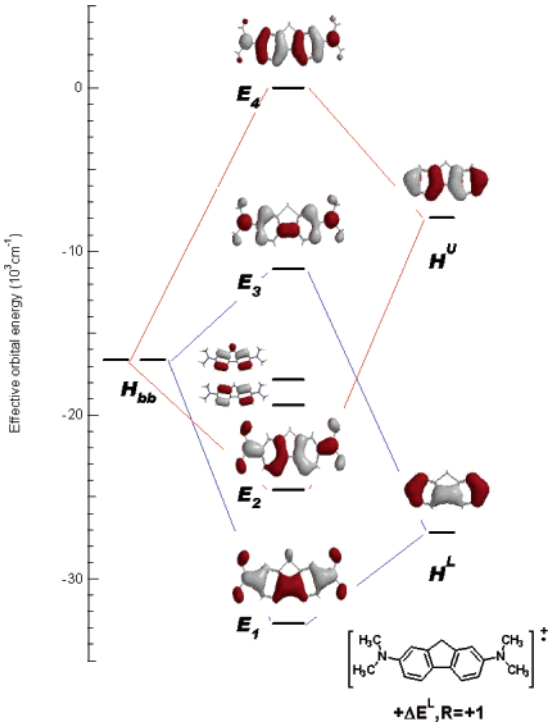

FIGURE 7. Adiabatic and diabatic energy pattern for the $R = +1$ neighboring orbital solution of **MBZ(CH₂)**$^+$.

As pointed out above, E_{a1} is $(E_4 - E_3)$, which is evaluated reasonably well for this series of compounds using Koopmans-based calculations (see Figure 4). According to the neighboring orbital analysis, this energy gap is given by eq 7.

$$(E_4 - E_3) = \frac{1}{2}(H^U - H^L) + \frac{1}{2}[(\Delta E^U)^2 + 4(V^U)^2]^{1/2} - \frac{1}{2}[(\Delta E^L)^2 + 4(V^L)^2]^{1/2} \quad (7)$$

It is determined by the diabatic energies as well as by the electronic couplings. The neighboring orbital analyses are quite similar for all the linked benzidine compounds, so we will focus on one compound, **MBZ(CH₂)**$^+$. The center of Figure 7 shows its adiabatic neighboring orbitals (E_1−E_4) obtained from the Koopmans-based calculations as well as the two noninteracting bridge π orbitals (corresponding to the a_u and b_{1g} orbitals of Figure 5) that lie between E_2 and E_3. These noninteracting orbitals have nodes through the CN bonds so they have essentially no interaction with the H_{bb} orbitals and are not part of the neighboring orbital system. The diabatic N-centered p orbitals H_{bb} are shown to the left, and the bridge H^U and H^L orbitals are shown to the right (fluorene orbitals are used as the illustrations) for what we argue below is the relevant neighboring orbital solution, for $R = +1$.

Equations 1−4 produce a range of possible diabatic energy/electronic coupling combinations. Real solutions to these equations are only obtained in a limited range of ΔE^L values, and the diabatic energies obtained plot linearly vs ΔE^L, as shown in Figure 8. When ΔE^L lies outside the range shown, the solutions are imaginary and not physically reasonable. The dependence of the electronic couplings V^U and V^L upon ΔE^L is shown in Figure 9. R becomes undefined when the diabatic charge-bearing unit pair energy H_{bb} crosses the lower diabatic energy H^L, which causes the discontinuity in the plot of R vs

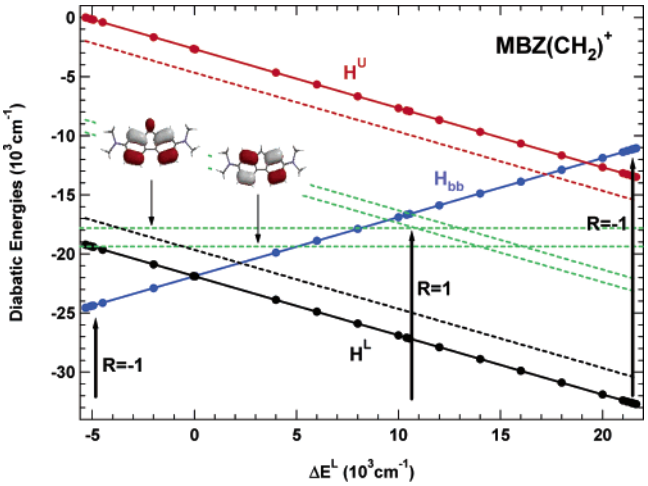

FIGURE 8. Plot of diabatic energies as a function of ΔE^L for the neighboring orbital treatment of **MBZ(CH₂)**$^+$.

ΔE^L, making solutions in this ΔE^L region unreasonable because $|R|$ is large. The most convincing evidence for which solutions within the range of real solutions are the most reasonable comes from considering the energies of noninteracting adiabatic aryl ring orbitals, which are shown as the horizontal dotted green lines for **MBZ(CH₂)**$^+$in Figure 8, along with electron density pictures. They are not part of the neighboring orbital system because they have nodes through the CN bonds and hence do not interact with the amino nitrogens. We also show orbital energies for the parent aromatic system, fluorene, arbitrarily plotted between the neighboring orbital H^U and H^L solutions as a function of ΔE^L, with the orbital corresponding to H^U shown as the red dashed line, the orbital corresponding to H^L shown as the black dashed line, and the orbitals corresponding to the noninteracting orbitals shown as the slanted green dashed lines. The only $|R| \sim 1$ solutions that have these noninteracting orbitals at reasonable energies relative to H^U and H^L are those near the $R = +1$ solution at $\Delta E^L \sim 10\ 600$ cm^{-1} (see the Supporting Information for more discussion). Although their values cannot be evaluated accurately because the $R = 1$ criterion is only an approximation, it is clear from these calculations that both electronic couplings V^U and V^L are substantial. The neighboring orbital calculations for the compounds studied here at $R = 1$ are summarized in Table 4. We note that the diabatic energies of the charge-bearing units, H_{bb}, in this case, the dialkylamino nitrogen p lone pair energies, ought to depend little upon the nature of the rather remote **X** linking unit. These diabatic energies are quite constant, falling in the range -15500 ± 600 cm^{-1}. It must be remembered that all of the diabatic energies are obtained relative to the adiabatic somo, but for this series of compounds, the orbitals involved are all very similar. The three terms of eq 7 are comparable in magnitude. As might be expected from this equation, there is not a significant correlation of $(E_4$−$E_3)$ with either of the electronic couplings (V^U or V^U); their average, ΔE^L; or the first term of eq 7, half the diabatic bridge orbital energy difference ($^1/_2(H^U - H^L)$) for calculations on **3BZ(X)** or **MBZ(X)** (the plots appear in Supporting Information). This suggests to us that it is not useful to consider the lowest transition energy for these compounds (or other Class III intervalence compounds) to be a direct measure of the electronic coupling. The changes in diabatic energies are about as important as the changes in couplings in determining the transition energy in this case.

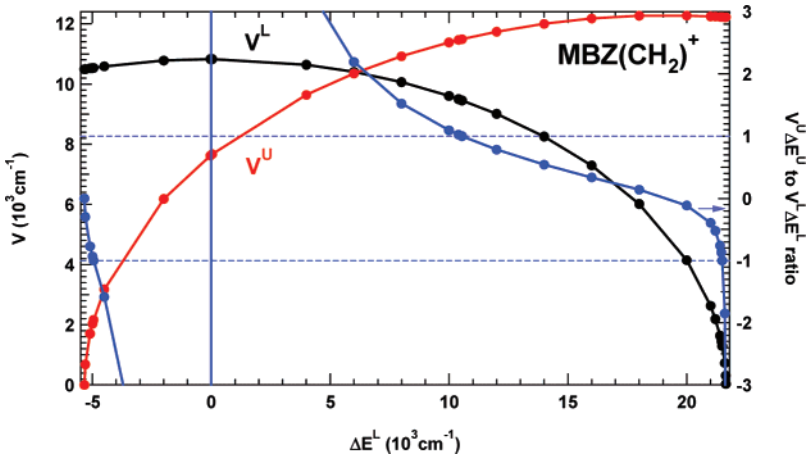

FIGURE 9. Plots of V values (left axis) and R (right axis) as a function of ΔE^L for the neighboring orbital treatment of **MBZ(CH$_2$)**$^+$.

TABLE 4. Neighboring Orbital Solutions at $R = +1$ for 3BZ(X)$^+$ (in cm^{-1})

compound	V^L	V^U	H^L	H_{bb}	H^U
3BZ(CH$_2$)$^+$	9290	11180	−26160	−16110	−7750
3BZ([CH$_2$]$_2$)$^+$	9330	10980	−25820	−15950	−7560
3BZ(HH)$^+$	9620	11170	−25090	−15840	−7880
3BZ(CO)$^+$	9580	11280	−25720	−16090	−7910
3BZ(NMe)$^+$	8350	11500	−25320	−15570	−8490
3BZ(S)$^+$	8600	11310	−24090	−15300	−8790
3BZ(SO$_2$)$^+$	8130	11470	−23360	−14870	−8850

Conclusions

The lowest-energy transition for delocalized intervalence compounds such as the **BZ(X)**$^+$ derivatives considered here has traditionally been called "the intervalence band". It is symmetry allowed and observed as a strong band in the spectrum that is separated rather well from other bands and shows vibrational fine structure so that its 0,0 band transition energy may be measured accurately. Although changes in the position of this band are calculated rather well using Koopmans-based calculations for the linked benzidines with both electron-withdrawing and -releasing **X** links, whether the higher energy transitions are calculated accurately enough to make the electronic couplings extracted from the adiabatic orbitals reasonably accurate is not easily tested experimentally. It is nevertheless clear that equating $E_{a1}/2$ with H_{ab} for mixing of the diabatic N orbitals with the bridge orbitals is too simplified to be very useful. There are not two but (at least) four energy levels that result from **M,B** interaction, so there is not the single excited state corresponding to **M,B** interaction that the two-state model assumes. There are separate electronic interactions for symmetric and antisymmetric nitrogen-centered orbitals, and E_{a1} is not a gap that corresponds directly to either electronic interaction. The two-state model employs an effective coupling between the charge-bearing unit diabatic orbitals. The neighboring orbital (four state) model enables us to break down this effective coupling into the different mixings of the symmetric and antisymmetric nitrogen-centered orbitals with the bridge orbitals of the same symmetry. The facts that the $E_1 \rightarrow E_4$ transition is too high in energy to measure experimentally because of bad overlap with other transitions and that the $E_2 \rightarrow E_4$ transition is essentially forbidden at the ground-state geometry for compounds in which the **B**−**M** bonds are directed nearly 180° relative to each other (as is typical for intervalence compounds) make accurate extraction of H_{ab} for delocalized intervalence compounds using only experimental data difficult. The analysis given above finds H_{ab} for **BZ(X)** to be over twice as large as an $H_{ab} = E_{a1}/2$ two-state estimate and to have essentially no correlation with structure because the diabatic energy gaps change with **X**. It is clear that the two-state model should not be expected to accurately interpret either the position or the intensity of what has traditionally been called "the intervalence band" of delocalized intervalence compounds.

Experimental Section

4,4′-Bis(9,9-azabicyclo[3.3.1]nonane-3-one)biphenyl (BZ(H,H)). Benzidine (3.68 g, 0.02 mol), 2,7-cyclooctadienone (5 g), and 20 mL of methanol were stirred for about one week at room temperature in a 100 mL round-bottom flask. The solid that formed was filtered, and the portion soluble in hot THF/ethanol was crystallized from THF/methanol, giving 0.5 g (0.6%) of **BZ(H,H)** (mp: 262−263 °C). ^{1}H NMR ($CDCl_3$) δ 7.55 (d, 4H), 7.05 (d, 4H), 4.5 (br.s, 4H), 2.68, (dd, 4H), 2.42 (d, 4H), 1.6−2.0 (m, 12H). The empirical formula $C_{28}H_{32}N_2O_2$ was established by MS.

2,7-Bis(9,9-azabicyclo[3.3.1]nonane-3-one)fluorene (BZ(CH$_2$)). 2,7-Diaminofluorene (0.98 g, 5 mol), 1.23 g (10 mmol) of 2,6-cyclooctanone, and 20 mL of CH_3OH were stirred in a 100 mL round-bottom flask for about one week. The solid that formed was filtered, and the portion soluble in hot THF/ethanol was crystallized from THF/methanol, giving 0.5 g (9%) of **(BZ(CH$_2$) (**mp: 277−278 °C). ^{1}H NMR ($CDCl_3$) δ 7.51 (d, $J = 8.0$ Hz, 2H), 6.91 (dd, $J = 8.0$ Hz, $J = 2.1$ Hz, 2H), 6.80 (d, $J = 2.1$ Hz, 4H), 4.58 (s, 2H), 3.4 (s, 4H), 2.68 (dd, 4H), 2.42 (d, 4H), 1.6−2.0 (m, 12H). The empirical formula $C_{29}H_{32}N_2O_2$ was established by MS.

2,7-Diamino-9,10-dihydrophenanthrene. A mixture of 1 mL of concentrated H_2SO_4 and 6 mL of concentrated HNO_3 was added dropwise over a 5 h period to 1.4 g of 9,10-dihydrophenanthrene in 5 mL of acetic acid and 25 mL of acetic anhydride that was cooled to 0−5 °C. After stirring at room temperature for another 24 h, 100 mL of water was added, and the solid was filtered and crystallized from ethyl acetate, giving 1.0 g (47.6%) of 2,7-dinitro-9,10-dihydrophenanthrene (mp: 223−224 °C, lit.[21] 222−223 °C). ^{1}H NMR ($CDCl_3$) δ 3.05 (br s, 4H), 7.94 (dd, $J = 2.3$ Hz, $J = 8.4$ Hz, 2H), 8.20 (d, $J = 2.3$ Hz, 2H), 8.23 (d, $J = 8.4$ Hz, $J = 2.3$ Hz, 2H). A solution of 2.8 g (12.4 mmol) of stannous chloride dihydrate in 2.5 mL of concentrated hydrochloric acid was added to a hot solution (70−80 °C) of 0.38 g (1.4 mmol) of 2,7-dinitro-9,10-dihydrophenanthrene in 13 mL of acetic acid and stirred for 20 min at this temperature. After evaporating HCl and HOAc,

(21) Nimura, S.; Kikuchi, O.; Ohana, T.; Yabe, A.; Kondo, S.; Kaise, M. *J. Phys. Chem. A* **1997**, *101*, 2083−2088.

aqueous NaOH was added at ice-water bath temperature, and the mixture was filtered and washed with brine. The solid was dispersed into water, and excess 40% aqueous sodium hydroxide was added. The mixture was filtered, washed with water, and dried to give 0.23 g (78.7%) of 2,7-diamino-9,10-dihydrophenanthrene (mp: 155−156 °C). The empirical formula $C_{14}H_{14}N_2$ was established by high-resolution MS.

2,7-Bis(9,9-azabicyclo[3.3.1]nonane-3-one)-9,10-dihydrophenanthrene (BZ([CH$_2$]$_2$)). A mixture of 3,7-diaminodibenzothiophene (0.23 g, 1.1 mmol), 2,7-cyclooctadieneone (0.3 g, 2.4 mmol), and 10 mL of CH_3OH was stirred for about one week at room temperature. The solid that formed was filtered, and the portion soluble in THF/ethanol was recrystallized from THF/methanol, giving 0.31 g (63%) of (**BZ([CH$_2$]$_2$))** (mp: 280−281 °C). ^{1}H NMR ($CDCl_3$) δ 7.51 (d, J = 8.1 Hz, 2H), 6.91 (dd, J = 8.1 Hz, J = 2.1 Hz, 2H), 6.80 (d, J = 2.1 Hz, 4H), 4.55 (s, 4H), 3.4 (s, 4H), 2.68 (dd, 4H), δ 2.42 (d, 4H), 1.6−2.0 (m,12H). The empirical formula $C_{30}H_{34}N_2O_2$ was established by MS.

2,7-Bis(9,9-azabicyclo[3.3.1]nonane-3-one)fluorenone (BZ-(CO)). 2,7-Diaminofluorenone (0.85 g, 4.1 mol), 2,6-cyclooctanone (1.1 g, 0.9 mmol), and 40 mL of ethanol were refluxed about one week. After filtration, the solid that formed was extracted with THF, and the residue after evaporation was recrystallized from methanol/ether, giving 0.5 g (9%) of **BZ(CO)** (mp: 282−283 °C). ^{1}H NMR ($CDCl_3$) δ 7.28 (d, J = 8.5 Hz, 2H), 7.24 (d, J = 2.7 Hz, 2H), 6.96 (dd, J = 8.5 Hz, J = 2.7 Hz, 2H), 4.5 (s, 4H), 2.68, (dd, 4H), 2.42 (d, 4H), 1.6−2.0 (m, 12H). The empirical formula $C_{29}H_{30}N_2O_3$ was established by MS.

2,7-Dinitro-*N*-methylcarbazole. To a solution of 0.5 g of 2,7-dinitrocarbazole[22] in 10 mL of acetone was added 0.5 g of KOH in 0.25 mL of water, and the reaction mixture was stirred at 50 °C for 20 min. When the reddish solution of the potassium salt of 2,7-dinitrocarbazole was obtained, dimethyl sulfate (1 mL, 8 mmol) was added. After stirring at 50 °C for another 20 min, the reaction mixture was cooled, diluted with water, and filtered. The solid was washed with water and dried in air, giving 0.51 g of 2,7-dinitro-*N*-methylcarbazole (mp: 160−161 °C). ^{1}H NMR ($CDCl_3$) δ 8.44 (d, J = 1.7 Hz, 2H), 8.26 (d, J = 8.6 Hz, 2H), 8.22 (dd, J = 8.6 Hz, J = 1.7 Hz), 4.05 (s, 4H).

2,7-Diamino-*N*-methylcarbazole. A solution of 2.1 g of $SnCl_2 \cdot H_2O$ in 1.5 mL of HCl was added dropwise to a hot solution (70−80 °C) of 0.29 g (1.1 mmol) of 2,7-dinitro-*N*-methylcarbazole in 3 mL of acetic acid. After refluxing for 3 h, solvent was evaporated and aqueous sodium hydroxide was added slowly, with cooling in an ice bath. After stirring for 0.5 h, the product was filtered, washed with water several times, and dried in air to give 0.2 g (90%) of 2,7-diamino-*N*-methylcarbazole (mp: 168−169 °C). ^{1}H NMR ($CDCl_3$) δ7.70 (d, J = 8.2 Hz, 2H), 6.63 (d, J = 1.4 Hz, 2H), 6.59 (dd, J = 8.2 Hz, J = 1.4 Hz), 3.79 (s, 4H), 3.65 (s, 3H).

2,7-Bis(9,9-azabicyclo[3.3.1]nonane-3-one)-*N*-methylcarbazole (BZ(NMe)). A mixture of 2,7-diamino-*N*-methylcarbazole (0.2 g, 0.9 mmol), 2,7-cyclooctadieneone (0.3 g, 2.4 mmol), and 20 mL of methanol was stirred for about one week at room temperature. After filtration, the portion soluble in THF/ethanol was crystallized from THF/methanol to give 0.25 g (60%) of **BZ(NMe) (**mp: 303−304 °C). ^{1}H NMR ($CDCl_3$) δ 7.82 (d, J = 8.6 Hz, 2H), 6.87 (dd, J = 8.5 Hz, J = 2.1, 2H), 6.84 (d, J = 2.1 Hz, 2H), 4.60 (s, 4H), 3.74 (s, 3H), 2.68 (dd, 4H), 2.42 (d, 4H), 1.6−2.0 (m, 12H). The empirical formula $C_{29}H_{33}N_3O_2$ was established by MS.

3,7-Dinitrodibenzothiophene-5-oxide. A solution of 23 g of 77% *m*-chloroperbenzoic acid (17.3 g, 0.1 mol) in 200 mL of chloroform was slowly added to a solution of 18.4 g of dibenzothiophene (0.1 mol) in 250 mL of chloroform at −30 to −35 °C. After stirring at −30 °C for 1 h, the mixture was stirred at room temperature for 1 h. Aqueous Na_2CO_3 was added dropwise into the mixure until the acid dissolved. The organic layer was washed twice with saturated $NaHCO_3$ and dried over Na_2SO_4, and after removal of solvent, the solid was recrystallized from ethanol, giving 18.2 g (91%) of white dibenzothiophene-9-oxide (mp: 187−188 °C, lit.[23] 187−189 °C). ^{1}H NMR ($CDCl_3$) δ 7.48−7.59 (m, 6H), −7.8 (m, 2H). A solution of 3 g (15 mmol) of this material in 70 mL of concentrated sulfuric acid was cooled to 6−12 °C, and 60 mL of concentrated nitric acid was added slowly so that the reaction temperature remained at 10−15 °C. The mixture was left at this temperature for 30 min and then allowed to come to room temperature over 30 min. The precipitate obtained by pouring the nitration mixture on ice was washed with water and air-dried to give 3.3 g (76%) of 3,7-dinitrodibenzothiophene-5-oxide as pale yellow crystals (mp: 257−258 °C, lit.[24] 257−258 °C). ^{1}H NMR ($CDCl_3$) δ 8.87 (d, J = 2.1 Hz), 8.61 (dd, J = 2.1 Hz, J = 8.6 2H), 8.12 (d, J = 8.6 Hz).

3,7-Bis(9,9-azabicyclo[3.3.1]nonane-3-one)dibenzothiophene (BZ(S)). A solution of 14.5 g (63 mmol) of stannous chloride dihydrate in 21 mL of concentrated hydrochloric acid was added to a hot solution (70−80 °C) of 1.66 g (5.8 mmol) of 3,7-dinitrodibenzothiophene-5-oxide in 30 mL of acetic acid and stirred for 2 h at room temperature. Then, the white suspension was heated at 100 °C and stirred for 1 h. After cooling to room temperature, the reaction mixture was filtered and washed with brine. The solid was dispersed into water, and excess 40% aqueous sodium hydroxide was added. The mixture was filtered, washed with water, and dried to give 1 g (81.6%) of 3,7-diaminodibenzothiophene as a pale yellow solid (mp: 172−173 °C, lit.[23] 172−173 °C). ^{1}H NMR ($CDCl_3$) δ 7.75 (d, J = 8.5 Hz, 4H), 7.06 (d, J = 2.2 Hz, 4H), 6.77 (dd, J = 8.5 Hz, J = 2.2 Hz). A mixture of this material (0.86 g, 4 mmol), 2,7-cyclooctadienone (1.1 g, 9 mmol), and 20 mL of methanol was stirred about one week at room temperature. The solid was filtered, and the portion soluble in THF/ethanol was recrystallized several times from THF/methanol, giving 1.1 g (60%) of **BZ(S)** (mp: 307−308 °C). ^{1}H NMR ($CDCl_3$) δ 7.91 (d, 8.8 Hz, 4H), 7.38 (d, J = 2.3 Hz, 4H), 7.12 (dd, J = 8.8 Hz, J = 2.3 Hz), 4.55 (s, 4H), 2.68, (dd, 4H), 2.42 (d, 4H), 1.6−2.0 (m,12H). The empirical formula $C_{28}H_{30}N_2O_2S$ was established by MS.

2,7-Dinitrodibenzothiophene Sulfone. A solution of 50 g of 77% *m*-chloroperbenzoic acid (38.5 g, 0.22 mol) in 200 mL of chloroform was slowly added to a solution of 18.4 g of dibenzothiophene (0.1 mol) in 250 mL of chloroform at room temperature, and the mixture was refluxed for 3 h. After the mixture cooled, aqueous sodium bicarbonate was added and the acid was dissolved. The chloroform solution was washed twice with saturated $NaHCO_3$, dried over Na_2SO_4, and concentrated. Recrystallization from ethanol gave 19.6 g (91%) of dibenzothiophene sulfone as a white solid (mp: 232−233 °C, lit.[25] 232−234 °C). A solution of 4 g (15 mmol) of dibenzothiophene sulfone in 70 mL of concentrated sulfuric acid was cooled to 6−12 °C, and 60 mL of concentrated nitric acid was added slowly so that the reaction temperature remained at 10−15 °C. The mixture was left at this temperature for 30 min and then allowed to come to room temperature over 30 min. After the mixture stirred at room temperature for 12 h, the precipitate was obtained by pouring the nitration mixture on ice and was collected on a Buchner funnel, washed with water, and air-dried to give 3.5 g (55%) of 3,7-dinitrodibenzothiophene sulfone as pale yellow crystals (mp: 253−254 °C, lit.[24] 257−258 °C). ^{1}H NMR ($CDCl_3$) δ 8.77 (d, J = 2.1 Hz, 2H), 8.6 (dd, J = 2.1 Hz, J = 8.4, 2H), 8.12 (d, J = 8.4 Hz, 2H).

3,7-Bis(9,9-azabicyclo[3.3.1]nonane-3-one)dibenzothiophene Sulfone (BZ(SO$_2$)). A solution of 10 g (45 mmol) of stannous chloride dihydrate in 8 mL of concentrated hydrochloric acid was added to a hot solution (70−80 °C) of 1.6 g (5 mmol) of 3,7-

(22) Morin, J.-F.; Leclerc, M. *Macromolecules* **2001**, *34*, 4680−4682.

(23) LaRochelle, R. W.; Trost, B. M. *J. Am. Chem. Soc.* **1971**, *93*, 6077−6086.

(24) Brown, R. K.; Nelson, N. A.; Wood, J. C. *J. Am. Chem. Soc.* **1952**, *74*, 1165−1167.

(25) LaCount, R. B.; Friedman, S. *J. Org. Chem.* **1977**, *42*, 2751−2754.

dinitrodibenzothiophene sulfone in 13 mL of acetic acid and stirred for 10 min at this temperature. After evaporating the solvent, aqueous NaOH was added at ice-water bath temperature, and the reaction mixture was filtrated and washed with brine. The solid was dispersed into water, and excess 40% aqueous sodium hydroxide was added. The mixture was filtered, washed with water, and dried to give 1.2 g (81.6%) of 3,7-diaminodibenzothiophene sulfone as a pale yellow solid (mp: 327−328 °C, lit.[24] 330−332 °C). ^{1}H NMR ($CDCl_3$) δ 3.77 (s, 4H), 6.76 (dd, J = 2.1 Hz, J = 8.4 Hz, 2H), 7.05 (d, J = 2.1 Hz, 2H), 7.74 (d, J = 8.4 Hz, 2H). A mixture of 0.86 g (4 mmol) of this material, 1.1 g (9 mmol) of 2,7-cyclooctadienone, and 20 mL of methanol was stirred about one week at room temperature, and the portion of the solid that formed that was soluble in hot THF/ethanol was recrystallized several times from THF/methanol, giving 1.1 g (60%) of **BZ(SO$_2$)** (mp: 309−310 °C). ^{1}H NMR ($CDCl_3$) δ 7.91 (d, J = 8.8 Hz, 4H), 7.38 (d, J = 2.3 Hz, 4H), 7.12 (dd, J = 8.8 Hz, J = 2.3 Hz), 4.55 (s, 4H), 2.68, (dd, 4H), 2.42 (d, 4H), 1.6−2.0 (m, 12H). The empirical formula $C_{28}H_{30}N_2O_4S$ was established by MS.

Calculations. Calculations were conducted using the 6-31G* and 6-31+G* basis sets as implemented in the Gaussian 98[26] program suite or Spartan 02.[27] Unrestricted Hartree−Fock calculations were requested for all doublet HF geometry optimizations. All geometry optimizations incorporated standard gradient methods. Frequency analyses were conducted on optimized geometries to confirm that the geometry resided on a minimum on the potential energy surface. All density functional calculations were completed using the B3LYP[28,29] density functional as implemented in Gaussian 98. The intensities of NCG and DCG transitions may be obtained from the dipole matrixes,[30,31] and the oscillator strengths are included in Table 2.

Absorption Spectroscopy. The radical cations were obtained by oxidation of the neutral compounds with tri(*p*-bromophenyl)-aminium hexachloroantimonate in acetonitrile, and the spectra were obtained at concentrations in the 10−50 μmol range at room temperature.

Acknowledgment. We thank NSF grant CHE-0240197 (SFN) and CHE-0507929 (JIZ) for partial financial support of this work and NSF Grant CHE-0091916 and gifts from the Intel Corporation for departmental computers used in this work.

Supporting Information Available: The complete citation for ref 26, calculated orbital energies, a Table like Table 2 for **MBZ-(CH$_2$)$^+$**, summaries of NCG and DCG calculations, plots of V vs ΔE^L, and Cartesian (xyz) coordinates for all **3BZ** and **MBZ** cation derivatives. This material is available free of charge via the Internet at http://pubs.acs.org.

JO060466L

(26) Frisch, M. J. et al. *Gaussian 98*, revision A.9; Gaussian, Inc.: Pittsburgh, PA, 1998.

(27) *Spartan 02*; Wavefunction Inc.: Irvine, CA.

(28) Becke, A. D. *J. Chem. Phys.* **1993**, *98*, 5648-5652.

(29) For references detailing the three-component functionals, see: (a) Becke, A. D. *Phys. Rev. A* **1988**, *38*, 3098−3100. (b) Lee, C.; Yang, W.; Parr, R. G. *Phys. Rev. B* **1988**, *37*, 785−789. (c) Vosko, S. H.; Wilk, L.; Nusair, M. *Can. J. Phys.* **1980**, *58*, 1200−1211.

(30) The dipole matrixes, which may be printed using the DIMO keyword in NBO,[31] contain the *x*, *y*, and *z* components of the transition dipole, μ_{12} (in atomic units; 1 au = 2.5418 D, the unit preferred by chemists). We converted the μ_{12} (D) values thus obtained to oscillator strengths, *f*, using $f = 1.085 \times 10^{-5} E_a$ (cm^{-1}) (μ_{12}(D)/4.8032)^2.

(31) Glendening, E. D.; Badenhoop, J. K.; Reed, A. E.; Carpenter, J. E.; Bohmann, J. A.; Morales, C. M.; Weinhold, F. *NBO 5.0*; Theoretical Chemistry Institute, University of Wisconsin: Madison, WI, 2001.